Canad. Math. Bull. Vol. **50** (4), 2007 pp. 547–566

Inverse Laplace Transforms Encountered in Hyperbolic Problems of Non-Stationary Fluid-Structure Interaction

Serguei Iakovlev

Abstract. The paper offers a study of the inverse Laplace transforms of the functions $I_n(rs)\{sI_n'(s)\}^{-1}$ where I_n is the modified Bessel function of the first kind and r is a parameter. The present study is a continuation of the author's previous work on the singular behavior of the special case of the functions in question, r=1. The general case of $r \in [0,1]$ is addressed, and it is shown that the inverse Laplace transforms for such r exhibit significantly more complex behavior than their predecessors, even though they still only have two different types of points of discontinuity: singularities and finite discontinuities. The functions studied originate from non-stationary fluid-structure interaction, and as such are of interest to researchers working in the area.

Introduction

We analyze the functions $\xi_n(r,t)$ for which the Laplace transforms are

$$\Xi_n(r,s) = \frac{\mathrm{I}_n(rs)}{s\,\mathrm{I}_n'(s)}, \tag{1}$$

where I_n is the modified Bessel function of the first kind, n is an integer, and $r \in [0,1]$. They are a two-dimensional generalization of the functions $\psi_n(t)$ which were addressed in [7], the Laplace transforms of which are

$$\Psi_n(s) = \frac{\mathrm{I}_n(s)}{s\,\mathrm{I}_n'(s)}. \tag{2}$$

Both functions appear in problems of mathematical physics involving the wave equation in cylindrical coordinates being solved using the Laplace transform technique applied to the time variable combined with separation of the spatial variables. Such methodology has proven to be efficient when one is concerned with analysis of the interaction between cylindrical structures and acoustical pulses or weak shock waves (*e.g.,* [4–6, 9]). The functions ξ_n and ψ_n can be referred to as the *response functions*, and knowing these functions reduces solving the respective fluid-structure interaction problems to a series of mostly routine computations.

The functions ψ_n allow one to compute the pressure on the surface of the structure, whereas their two-dimensional counterparts ξ_n allow for simulation of the entire hydrodynamic field inside the structure, r being the dimensionless radial distance

Received by the editors July 5, 2005.
AMS subject classification: Primary: 44A10; secondary: 44A20, 33C10, 40A30, 74F10, 76Q05.

in cylindrical coordinates. Since the latter provides the researcher with qualitatively different information about the interaction between structures and hydrodynamic loads, analysis of the functions ξ_n and developing efficient algorithms for their numerical evaluation seems to be of considerable applied value. Specifically, knowing the functions ξ_n will allow for obtaining high-accuracy converged analytical solutions for rather complex non-stationary problems of fluid-structure interaction. Such solutions can be successfully used as benchmarks for verification of various numerical codes [10].

The one-dimensional counterparts, ψ_n, were found to have infinitely many regularly distributed singular points of two different types [7], an irregular behavior that definitely deserved some attention. Since the functions ξ_n are closely related to ψ_n, it seems reasonable to suggest that their behavior is at least as irregular as that of ψ_n. However, to the best of the author's knowledge, the functions ξ_n have not yet been addressed. It therefore appears to be of theoretical interest to establish their main features, especially in light of the discontinuous nature of their one-dimensional counterparts. Of special interest here is the analysis of the effect that a seemingly insignificant change (multiplying the argument of the Bessel function in the numerator of (2) by a parameter r) has on the behavior of the functions.

It should be mentioned that the approach where certain functions independent of the physical parameters of the system modelled are considered as separate mathematical entities was first introduced in the fluid-structure interaction context by Geers [4] who considered an external hydrodynamic loading on a circular cylindrical shell. The present work can therefore be seen as part of an attempt to extend the now classical methodology to make it applicable to a wider variety of problems, specifically to studies where entire hydrodynamic fields are simulated, not only surface pressures. Along with two-dimensional simulations, such an extension enables one to model three-dimensional non-stationary hydrodynamic fields induced by the interaction between fluids and structures, at least theoretically (see [8] for information on obtaining three-dimensional solutions using the corresponding two-dimensional ones).

Series Representation of Inverses

The analytical inversion procedure based on the application of the residue theory to Mellin's integral for Ξ_n can be successfully used to obtain the inverses of (1). Since Ξ_n has the same denominator as Ψ_n, we can utilize some of the results obtained earlier [7]. Specifically, the functions Ξ_n can be shown to have infinitely many pure imaginary simple poles given by

$$s^n_{\pm k} = \pm i\omega^n_k, \quad k = 1, 2, \dots, \tag{3}$$

where ω^n_k is the k-th positive zero of the derivative of J_n, the Bessel function of the first kind of order n. Furthermore, $s = 0$ can be shown to be a removable singular point for Ξ_n when $n \geq 1$ and a second order pole when $n = 0$.

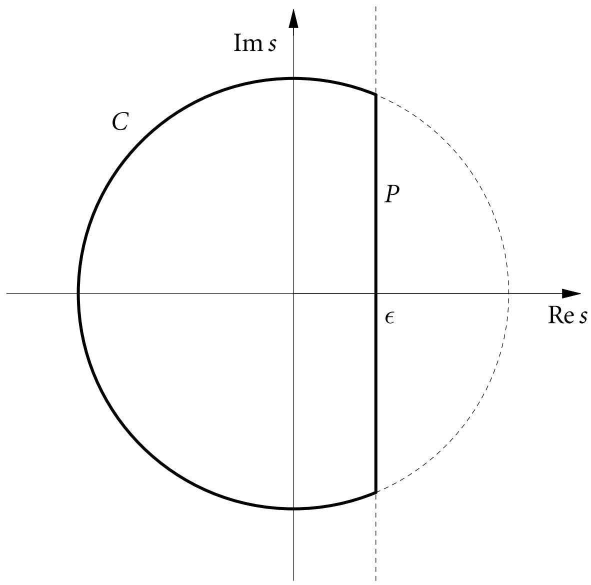

Figure 1: The integration contour Γ.

Mellin's integral for Ξ_n^i is

$$\xi_n(r,t) = \frac{1}{2\pi i}\int_{\epsilon-i\infty}^{\epsilon+i\infty} \Xi_n(r,s)\, e^{st}\; ds, \tag{4}$$

where ϵ is such that all the singular points of the integrand $Z_n(r,s,t) = \Xi_n(r,s)\; e^{st}$ lie in the half-plane $\operatorname{Re} s < \epsilon$ (since all the singularities of $Z_n(r,s,t)$ are pure imaginary, any positive ϵ satisfies this condition). We consider a simple closed curve Γ consisting of the segment P of the line $\operatorname{Re}\, s = \epsilon$ and the arc C of the circle of radius R (Figure 1) and apply Cauchy's residue theorem to obtain ξ_n in terms of the residues of $Z_n(r,s,t)$. If Γ is such that it does not pass through any of the poles defined by (3), we have

$$\int_C Z_n(r,s,t)\, ds + \int_P Z_n(r,s,t)\, ds = 2\pi i \sum_{s_k^n \in D} R_{s_k^n}^n, \tag{5}$$

where $R_{s_k^n}^n$ is the residue of Z_n at the point s_k^n and D is the domain bounded by Γ. Normally, the next step would be to apply Jordan's lemma to show that the first integral on the left-hand side of (5) tends to zero as $R \to \infty$. However, in the present case the integrand has infinitely many poles (Figure 2) and Jordan's lemma cannot be used. To get around this difficulty, we will apply Jordan's modified lemma [7], but first we will consider ξ_n on a circle of a large radius R.

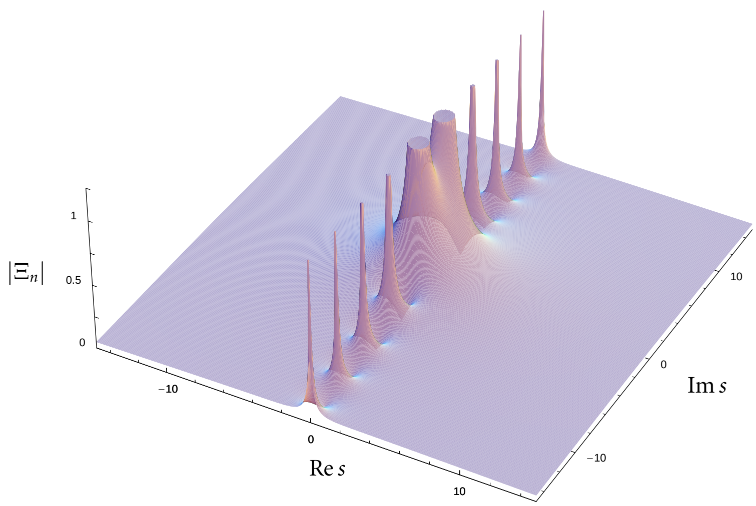

Figure 2: Poles of $\Xi_n(r,s)$ in the proximity of the origin.

Using the asymptotic expansions of $I_n(s)$ and $I_n'(s)$ for large $|s|$,

$$I_n(s) = \frac{1}{\sqrt{2\pi s}} \left(e^s + (-1)^n i\, e^{-s}\right)\left(1 + O(s^{-1})\right),$$
$$I_n'(s) = \frac{1}{\sqrt{2\pi s}} \left(e^s - (-1)^n i\, e^{-s}\right)\left(1 + O(s^{-1})\right),$$

respectively [3], we have

$$\Xi_n \sim \frac{e^{rs} + (-1)^n i\, e^{-rs}}{s(e^s - (-1)^n i\, e^{-s})}, \quad |rs| \gg 1.$$

From here on we assume that n is even. The case of odd n can be addressed in a very similar manner (even though the function χ introduced below will be slightly different in that case, the approach to obtaining estimates for χ outlined in Appendix A remains the same, as do the estimates themselves). If we express s in polar form $s = R\, e^{i\phi}$, we obtain

$$|\Xi_n| \sim \frac{1}{R}\chi(r, R, \phi), \tag{6}$$

where

$$\chi(r, R, \phi) = \left\{ \frac{e^{2rR\cos\phi} + e^{-2rR\cos\phi} + 2\sin(2rR\sin\phi)}{e^{2R\cos\phi} + e^{-2R\cos\phi} - 2\sin(2R\sin\phi)} \right\}^{\frac{1}{2}}.$$

https://doi.org/10.4153/CMB-2007-053-1 Published online by Cambridge University Press

Now we choose a family of circles that does not pass through any of the poles of Ξ_n or close proximities of them. The family

$$R_k = \pi k, \quad k = 1, 2, \dots, \tag{7}$$

for example, satisfies this condition, which can be shown by comparing (7) with the asymptotic formulae for the zeros of J'_n (see [1]). From here on, we consider the family of contours Γ_k constructed from the arcs C_k of radii R_k and corresponding segments.

It can be shown (Appendix A) that χ is uniformly bounded on the family of circles (7). Then it follows from (6) that the functions $\Xi_n(r, s)$ uniformly tend to zero (with respect to $\arg s$) on the infinite family of arcs C_k, and hence Jordan's modified lemma can be applied to demonstrate that $\lim_{k\to\infty} \int_{C_k} Z_n(r, s, t)\, ds = 0$. Then, considering the limit of (5) when $k \to \infty$ and $\Gamma = \Gamma_k$ and recalling Mellin's integral (4), the following residual expression for ξ_n can be obtained,

$$\xi_n(r, t) = \sum_{k=\pm 1, \pm 2, \dots} R^n_{s^n_k},$$

where s^n_k are the poles defined by (3) as well as $s = 0$ for $n = 0$.

It can be easily shown that the residues of $Z_n(r, s, t)$ at $s = 0$ and the poles $s = s^n_k$ are given by

$$R^0_0 = 2t,$$

$$R^n_{i\omega^n_k,\ k=1,2,\dots} = \frac{J_n(r\omega^n_k)}{J_n(\omega^n_k)} \frac{i\omega^n_k}{\{n^2 - (\omega^n_k)^2\}} \left\{\cos(\omega^n_k t) + i \sin(\omega^n_k t)\right\},$$

$$R^n_{-i\omega^n_k,\ k=1,2,\dots} = -\frac{J_n(r\omega^n_k)}{J_n(\omega^n_k)} \frac{i\omega^n_k}{\{n^2 - (\omega^n_k)^2\}} \left\{\cos(\omega^n_k t) - i \sin(\omega^n_k t)\right\}.$$

Then the following series representation of $\xi_n(r, t)$ can be obtained,

$$\xi_0(r, t) = 2t + 2 \sum_{k=1}^{\infty} \frac{J_0(r\omega^0_k)}{J_0(\omega^0_k)} \frac{1}{\omega^0_k} \sin(\omega^0_k t), \tag{8}$$

$$\xi_n(r, t) = 2 \sum_{k=1}^{\infty} \frac{J_n(r\omega^n_k)}{J_n(\omega^n_k)} \frac{\omega^n_k}{\{(\omega^n_k)^2 - n^2\}} \sin(\omega^n_k t), \quad n \geq 1. \tag{9}$$

The series expressions (8) and (9) appear to be very similar to those for the functions ψ_n [7]. This similarity, however, is not at all indicative of the nature of the functions ξ_n. As we will demonstrate shortly, the ξ_n exhibit much more complex behaviour than their one-dimensional counterparts ψ_n, and computational challenges one is faced with evaluating ξ_n and/or using them in subsequent computations are numerous and sometimes rather non-trivial.

Before we analyze any specific details, the following fundamental questions have to be answered. Do the functions ξ_n have points of discontinuity as their one-dimensional counterparts did? If yes, what are the types of those discontinuities, their number, and their location? If there are any points of finite discontinuity, what is the behaviour of ξ_n in the proximity of those points and what are the magnitudes of the finite discontinuities? The following two sections address these questions.

Series Convergence and Singular Points

To study the convergence of the series (9), we first consider the general term of (9),

$$\gamma_k(n,r,t) = 2\,\alpha_k^n(r)\,\frac{\omega_k^n}{((\omega_k^n)^2 - n^2)}\sin(\omega_k^n t),$$

where

$$\alpha_k^n(r) = \frac{J_n(r\omega_k^n)}{J_n(\omega_k^n)},$$

at large k. Recalling [1] that

$$\omega_k^n = \beta_k^n - \frac{\mu+1}{8\beta_k^n} + O\Big(\frac{1}{k^3}\Big), \quad k \gg 1,$$

where $\mu = 4n^2$ and $\beta_k^n = \left(k + \frac{n}{2} - \frac{3}{4}\right)\pi$, and that

$$J_n(z) = \sqrt{\frac{2}{\pi z}}\cos\Big(z - \frac{n\pi}{2} - \frac{\pi}{4}\Big) + O\Big(\frac{1}{z^{\frac{3}{2}}}\Big),$$

the following asymptotic expressions can be obtained,

$$J_n(\omega_k^n) = \sqrt{\frac{2}{\pi\beta_k^n}}(-1)^{k-1} + O\Big(\frac{1}{k^{\frac{3}{2}}}\Big),$$

$$J_n(r\omega_k^n) = \sqrt{\frac{2}{\pi r\beta_k^n}}(-1)^{k-1}\cos(\beta_k^n(r-1)) + O\Big(\frac{1}{k^{\frac{3}{2}}}\Big).$$

Then

$$\alpha_k^n(r) = \frac{1}{\sqrt{r}}\cos(\beta_k^n(r-1)) + O\Big(\frac{1}{k}\Big), \quad k \gg 1, \tag{10}$$

and it can also easily be shown that

$$\frac{\omega_k^n}{((\omega_k^n)^2 - n^2)} = \frac{1}{\pi k} + O\Big(\frac{1}{k^2}\Big), \quad k \gg 1, \tag{11}$$

$$\sin(\omega_k^n t) = \sin(\beta_k^n t) + O\Big(\frac{1}{k}\Big). \tag{12}$$

Hence,

$$\gamma_k = \frac{\cos(\beta_k^n(r-1))\sin(\beta_k^n t)}{\sqrt{r}\pi k} + O\Big(\frac{1}{k^2}\Big), \quad k \gg 1, \tag{13}$$

https://doi.org/10.4153/CMB-2007-053-1 Published online by Cambridge University Press

and the N-th remainder of the series in (9) can be written as

$$2\sum_{k=N}^{\infty} \frac{J_n(r\omega_k^n)}{J_n(\omega_k^n)} \frac{\omega_k^n}{\{(\omega_k^n)^2 - n^2\}} \sin(\omega_k^n t) = I_1 + I_2,$$

where

$$I_1 = \frac{2}{\pi\sqrt{r}} \sum_{k=N}^{\infty} \frac{\cos(\beta_k^n(r-1))\sin(\beta_k^n t)}{k}, \tag{14}$$

$$I_2 = \sum_{k=N}^{\infty} O\Big(\frac{1}{k^2}\Big), \tag{15}$$

and it is assumed that $N \gg 1$. The series I_2 is absolutely convergent for any n on any finite t-interval. The convergence of the series I_1, however, needs to be studied. To do so, we rewrite (14) as $I_1 = G_1 + G_2$, where

$$G_1 = \frac{1}{\pi\sqrt{r}} \sum_{k=N}^{\infty} \frac{\sin(\beta_k^n(t+r-1))}{k}, \quad G_2 = \frac{1}{\pi\sqrt{r}} \sum_{k=N}^{\infty} \frac{\sin(\beta_k^n(t-r+1))}{k},$$

and analyze the series G_1 and G_2. By virtue of Dirichlet's test, G_1 and G_2 converge for all t except for the points

$$t_1^s = 2(2j+1) - r + 1, \quad j = 0, 1, \ldots, \tag{16}$$

$$t_2^s = 2(2j+1) + r - 1, \quad j = 0, 1, \ldots, \tag{17}$$

respectively. (Owing to the physics of the problems from which the functions ξ_n originate, we are only interested in non-negative values of t.) Therefore, the series I_1 diverges at t defined by (16) and (17), and so does the series in (9), which implies that the functions ξ_n have singularities at the points t_1^s and t_2^s. A few initial t-values given by (16) and (17) are $1+r$, $3-r$, $5+r$, $7-r$, $9+r$, $11-r$, $\ldots$. The values at the singular points follow a regular pattern which depends on n. Specifically, the singular points form pairs which produce infinity of the same sign, and the pairs producing positive infinity alternate with those producing negative infinity. For odd n, the first pair of singular points produces negative infinity, *i.e.,* one observes the following pattern,

$$\begin{array}{lccccccc} t: & 1+r & 3-r & 5+r & 7-r & 9+r & 11-r & \ldots \\ \xi_n(r,t): & -\infty & -\infty & \infty & \infty & -\infty & -\infty & \ldots \end{array}. \tag{18}$$

For even n the first pair produces positive infinity, *i.e.,* the pattern is

$$\begin{array}{lccccccc} t: & 1+r & 3-r & 5+r & 7-r & 9+r & 11-r & \ldots \\ \xi_n(r,t): & \infty & \infty & -\infty & -\infty & \infty & \infty & \ldots \end{array}. \tag{19}$$

Finite Discontinuities

Even though G_1 and G_2 converge at all t other than (16) and (17), it is possible that they have finite discontinuities. Namely, when t is such that all terms in G_1 or G_2 are zero, the respective series obviously converges to zero. However, the side limits of G_1 or G_2 at such t may differ from zero, which would imply that ξ_n has finite discontinuities at the points in question. Since $\sin(\beta_k^n(t+r-1)) = 0$ when

$$t = t_1^f = 4m - r + 1, \quad m = 0, 1, \dots, \tag{20}$$

and $\sin(\beta_k^n(t-r+1)) = 0$ for

$$t = t_2^f = 4(m+1) + r - 1, \quad m = 0, 1, \dots \tag{21}$$

(we are still only interested in positive values of t), the points t_1^f and t_2^f should be analyzed as potential points of finite discontinuity of ξ_n.

We note that the set (20) only produces the zero general term for the series G_1 and not for G_2. This can be shown as follows. The set (20) will produce the zero general term for G_2 if

$$r = 2l + 1, \quad l = 0, 1, \dots, \tag{22}$$

which means that r would have to be not only an integer but also odd. We are only considering $r \in [0, 1]$, and the only value that satisfies (22) is $r = 1$. Such r, however, implies that we are dealing with the functions ψ_n addressed earlier [7] (setting $r = 1$ reduces $\xi_n(r, t)$ to $\psi_n(t)$), and there is no need for the present analysis. In a similar fashion it can be shown that (21) does not produce the zero general term of G_1 for the values of r of interest. We have therefore demonstrated that at any given value of t only one of the series G_1 and G_2 can potentially be a source of finite discontinuity of ξ_n, a rather important fact that ensures that any finite discontinuity of G_1 or G_2 is that of ξ_n.

To determine whether ξ_n are discontinuous at the points t_1^f and t_2^f, we analyze the behaviour of the series G_1 and G_2 in the close proximity of those points. We first consider G_1 and assume that $t = 4m - r + 1 \pm \delta$, $0 < \delta \ll 1$. Then

$$G_1\big|_{t=4m-r+1\pm\delta} = \pm\frac{(-1)^m}{\pi\sqrt{r}} Q(\delta, N), \tag{23}$$

where

$$Q(\delta, N) = \sum_{k=N}^{\infty} \frac{\sin\left(\delta\pi\left(k + \frac{n}{2} - \frac{3}{4}\right)\right)}{k}.$$

The function Q can be expressed in terms of the Lerch transcendental function Φ [2, 7], where

$$\Phi(z, p, a) = \sum_{k=0}^{\infty} \frac{z^k}{(a+k)^p},$$

as

$$Q(\delta, N) = \frac{e^{i\delta\pi\left(N+\frac{n}{2}-\frac{3}{4}\right)}}{2i}\Phi(e^{i\delta\pi}, 1, N) - \frac{e^{-i\delta\pi\left(N+\frac{n}{2}-\frac{3}{4}\right)}}{2i}\Phi(e^{-i\delta\pi}, 1, N).$$

If we recall [2] that $\Phi(z, 1, a) \sim -\log(1-z)$ as $z \to 0$, it can be easily established that

$$Q(\delta, N) \to \frac{\pi}{2} \quad \text{as } \delta \to 0. \tag{24}$$

Then it follows from (23) and (24) that G_1 has different side limits at the points t_1^f, namely

$$\lim_{t\to(4m-r+1)^-} G_1 = -\frac{(-1)^m}{2\sqrt{r}}, \tag{25}$$

$$\lim_{t\to(4m-r+1)^+} G_1 = \frac{(-1)^m}{2\sqrt{r}}. \tag{26}$$

In a similar manner it can be shown that G_2 has finite discontinuities at the points t_2^f, namely

$$\lim_{t\to(4(m+1)+r-1)^-} G_2 = \frac{(-1)^m}{2\sqrt{r}}, \tag{27}$$

$$\lim_{t\to(4(m+1)+r-1)^+} G_2 = -\frac{(-1)^m}{2\sqrt{r}}. \tag{28}$$

Thus, we have shown that the series I_1 has finite discontinuities at the points t_1^f and t_2^f. The functions ξ_n, however, are also determined by the finite series I_0,

$$I_0 = 2\sum_{k=1}^{N-1} \frac{J_n(r\omega_k^n)}{J_n(\omega_k^n)} \frac{\omega_k^n}{\{(\omega_k^n)^2 - n^2\}} \sin(\omega_k^n t),$$

and the infinite series I_2. The series I_0 is a continuous function of t, so it does not contribute to the discontinuous nature of ξ_n. Is it possible that I_2 has discontinuities? The answer to this question is no (Appendix C). Thus, we have shown that I_1 is the only source of finite discontinuity of ξ_n, and we can state now that ξ_n have an infinite number of points of finite discontinuity at t defined by (20) and (21). We have also demonstrated that the magnitudes $L = 1/\sqrt{r}$ of those discontinuities are independent of the parameters t, n, and N.

Furthermore, we have established that, regardless of n, all ξ_n follow the same pattern in terms of the behaviour in the proximity of the points of finite discontinuity. Except for the first point of the set (20), all other points defined by (20) form pairs with the neighboring points defined by (21), and the points of each pair produce the same difference between the left- and right-side limits of ξ_n. Specifically, the first point of the set (21), $3 + r$, and the second point of the set (20), $5 - r$, form a pair such that the difference between the left- and right-side limits of ξ_n is positive at both points. The second point of the set (21), $7 + r$, and the third point of the set (20), $9 - r$, produce a pair such that the difference between the left- and right-side limits is negative, and so on. This pattern can be summarized as follows,

$$\begin{array}{cccccccccc} t_f: & 1-r & 3+r & 5-r & 7+r & 9-r & 11+r & 13-r & \dots \\ L: & -\frac{1}{\sqrt{r}} & \frac{1}{\sqrt{r}} & \frac{1}{\sqrt{r}} & -\frac{1}{\sqrt{r}} & -\frac{1}{\sqrt{r}} & \frac{1}{\sqrt{r}} & \frac{1}{\sqrt{r}} & \dots \end{array}$$

where $L = \lim_{t \to t_f^-} \xi_n(r,t) \; - \lim_{t \to t_f^+} \xi_n(r,t)$ is the difference between the left- and right-side limits of ξ_n at t_f. We note that the first point of the set (20), $t_f = 1 - r$, is "unique" in a sense that it has no pair, and that the magnitude of this very first finite discontinuity is still $1/\sqrt{r}$.

At the points of finite discontinuity, $I_1 = 0$ and the value of ξ_n is completely determined by two continuous functions, I_0 and I_2. Recalling (25)–(28), it can be easily shown that

$$\xi_n(r,t)|_{t=t_f} = \frac{1}{2}\left\{ \lim_{t \to t_f^-} \xi_n(r,t) + \lim_{t \to t_f^+} \xi_n(r,t) \right\}, \tag{29}$$

where t_f is any of the points of finite discontinuity defined by (20) and (21).

Thus, we have demonstrated that the functions ξ_n have infinitely many singularities and infinitely many points of finite discontinuity that form a regular pattern in which pairs of singularities alternate with the pairs of finite discontinuities. The locations of the points of discontinuity, t_d, are given by (16), (17), (20), and (21) and can be described by one equation, $t_d = (2j + 1) \pm r$, $j = 0, 1, \dots$. The distribution of discontinuities can be summarized as follows, S standing for singular points and F for points of finite discontinuity,

$$\begin{array}{cccccccccc} 1-r & 1+r & 3-r & 3+r & 5-r & 5+r & 7-r & 7+r & 9-r & \dots \\ F & S & S & F & F & S & S & F & F & \dots \end{array}$$

Numerical Results

Having understood the most important features of the functions ξ_n, we will now look at their graphs for various r and n. We start with $n = 1$ and $r = 0.5$ (Figure 3). The pattern of discontinuities discussed can be clearly identified in the figure. The pairs of points of finite discontinuity alternate with singular points except for the first finite discontinuity at $t = 1 - r = 0.5$. The sign of the infinity is the same for each pair of singularities and it alternates between the pairs. The finite discontinuities always have the same magnitude of $1/\sqrt{0.5} = 1.41\dots$, and the sign of the difference between the left- and right-side limits is the same for both points of each pair, and it alternates between the pairs as well. The solid dots show the values of ξ_n at the points of finite discontinuity which are given by (29). We mention that the presence of finite discontinuities and singularities has a clear physical interpretation in the

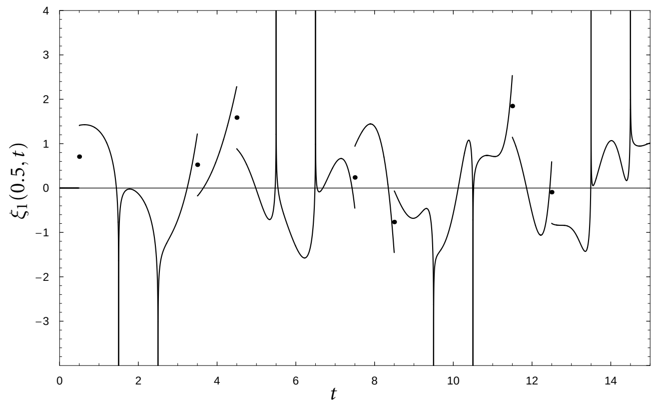

Figure 3: Function $\xi_1(0.5, t)$.

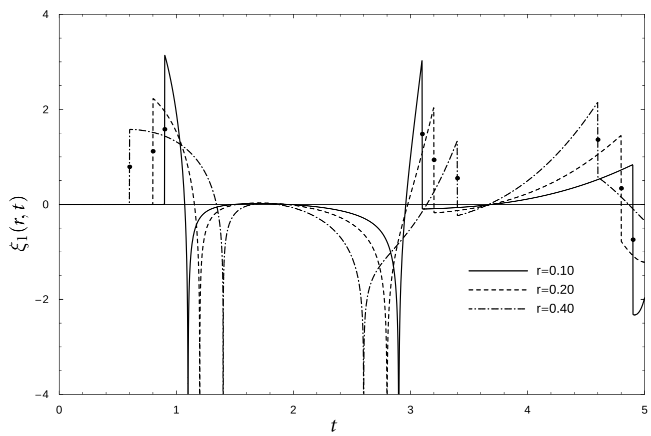

Figure 4: Function $\xi_1(r, t)$ for $r = 0.10$, 0.20, and 0.40.

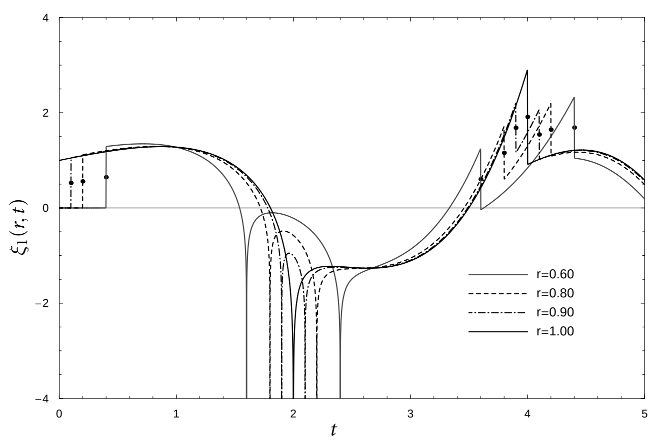

Figure 5: Function $\xi_1(r, t)$ for $r = 0.60$, 0.80, 0.90, and 1.00.

https://doi.org/10.4153/CMB-2007-053-1 Published online by Cambridge University Press

context of the corresponding fluid-structure interaction problems (*e.g.,* [9]). This aspect, however, is beyond the scope of this paper.

Now we focus on the influence of r on the appearance of ξ_n, and consider $\xi_1(r,t)$ for various r, (Figures 4 and 5; to make the graphs easier to visualize, the functions are shown as continuous, with dots still representing the values at the points of finite discontinuity). Even though the sequence of the discontinuities remains the same for all r, their location changes depending on r. Specifically, the closer r is to unity the closer any two neighboring discontinuities of the *same type* (either two singularities or two finite discontinuities) are to each other, except for the very first one. Eventually (at $r = 1$) they merge to form one point of discontinuity of the respective type. As r becomes smaller and smaller, any two neighboring discontinuities of *different type* are getting closer and closer to each other and eventually merge at $r = 0$ to produce a discontinuity point of "mixed" nature with a singularity on one side and a finite discontinuity on the other (not shown, see Appendix C).

It appears so far that for the n and r values considered, the computational challenges one faces dealing with the "irregularity" of the functions ξ_n should not be any different from those encountered for the functions ψ_n: even though the number of points of discontinuity is different, we are still dealing with piecewise smooth functions defined on a (infinite) set of finite intervals. This seeming similarity vanishes as r decreases and n increases. To demonstrate what exactly is happening and to show clearly the difference between $\xi_n(r,t)$ for the same n but different r, we look at the graphs of ξ_n for $r = 0.2$ and $n = 5$ and 20, and compare those to the graphs of ψ_n at the same two values of n, (Figures 6 and 7; $\psi_n(t) = \xi_n(1,t)$). First of all, it is clear that even if n remains unchanged, decrease of r leads to a significantly less regular behaviour of ξ_n. Specifically, instead of being relatively evenly distributed along the real axis, the "mass" of the function tends to accumulate in the intervals formed by any two neighboring points of discontinuity of different type, and outside those intervals the values of the function are very close to zero. This tendency becomes more and more pronounced as n increases, and even for a relatively small value of $n = 20$, one observes a pattern where high-frequency intervals alternate with those where the function has a constant value (zero or almost so). We mention that the frequency inside the "problem" intervals is not uniformly distributed and increases significantly as t approaches the ends of the intervals, *i.e.,* the points of discontinuity.

The phenomena mentioned are a clear indication of the fact that one has to deal with much more challenging numerical difficulties computing ξ_n than was the case for ψ_n. The most dramatic and computationally challenging scenario occurs when r is very small and n is very large. As an example, Figure 8 shows $\xi_{150}(0.02,t)$. This is an extremely interesting and beautiful function. It is zero virtually everywhere except for an infinite number of very narrow intervals where it oscillates with extremely high frequency. Inside the high-frequency intervals (insets 1 and 2), the frequency of oscillations is not uniform and it continuously increases as t approaches the ends of the intervals. In the close proximity of the ends it becomes so high that it is possible to define the "ultra-high-frequency" regions, insets 3 and 4. The frequency of oscillation in the ultra-high-frequency intervals can be as much as 20 times higher than that in the high-frequency ones. It is important to mention that in spite of the very high frequency of oscillations, their magnitude is still finite throughout the intervals in

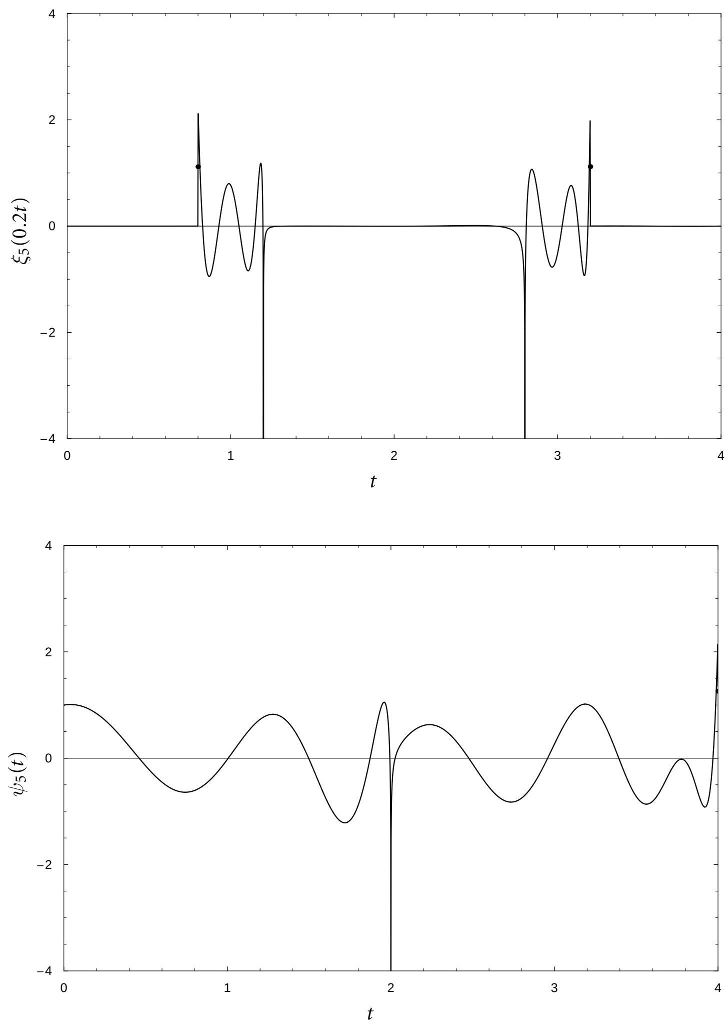

Figure 6: Functions $\xi_5(0.2, t)$ and $\psi_5(t)$.

questions. The singular points visible in Figure 8 are located at $t = 1.02$ and 2.98, and finite discontinuities with the magnitude of $1/\sqrt{0.02} = 7.07\ldots$ occur at $t = 0.98$, 3.02, and 4.98.

Conclusions

An analytical inversion procedure based on the use of the residue theory was applied to obtain the series expressions for the functions $\xi_n(r, t)$, and the convergence of those series was studied. It was demonstrated that the functions ξ_n have infinitely many points of discontinuity of two types, namely singular points and points of fi-

https://doi.org/10.4153/CMB-2007-053-1 Published online by Cambridge University Press

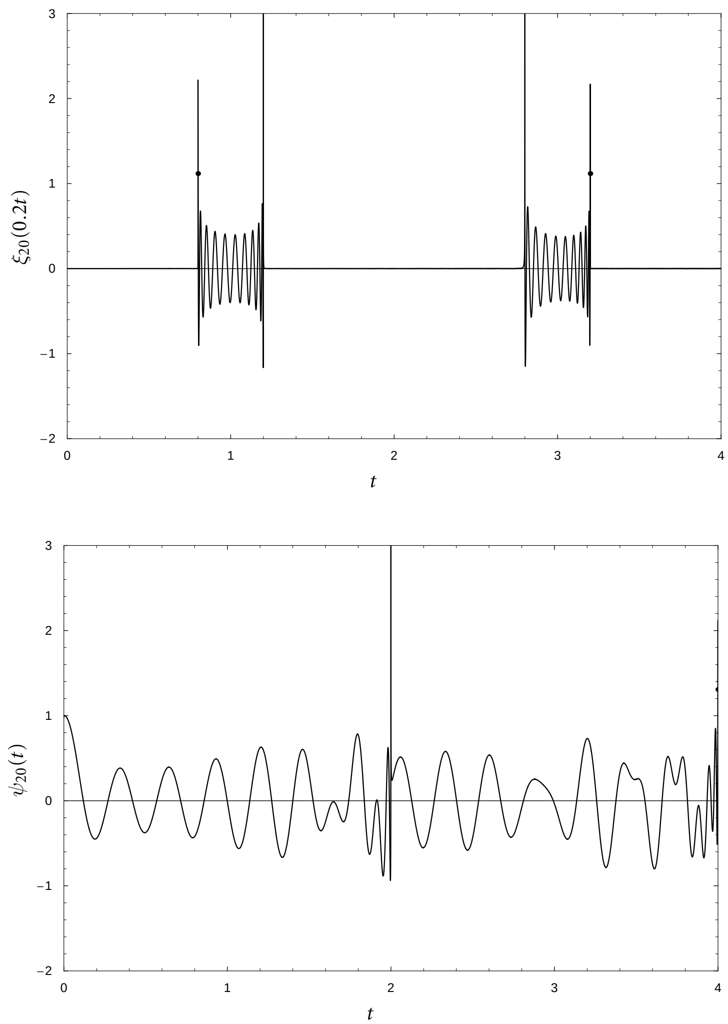

Figure 7: Functions $\xi_{20}(0.2, t)$ and $\psi_{20}(t)$.

nite discontinuity. Unlike the case of the functions ψ_n, which are a special case of ξ_n at $r = 1$, the location of the points of discontinuity of ξ_n is not fixed and changes depending on r, as do the magnitudes of the finite discontinuities. The latter always remains equal to $r^{-0.5}$ regardless of n and t, and any two consecutive points of finite discontinuity, except for the first one, form a pair such that ξ_n exhibits similar behaviour in the proximity of the both points. Consecutive singular points form pairs as well, and the points of each pair produce the infinity of the same sign. The signs of the infinity alternate between the pairs of singularities. For any $r \in (0, r)$, on any given t-interval the functions ξ_n have at least twice as many points of discontinuity as the functions ψ_n. In the case of $r = 0$, the number of points of discontinuity of

https://doi.org/10.4153/CMB-2007-053-1 Published online by Cambridge University Press

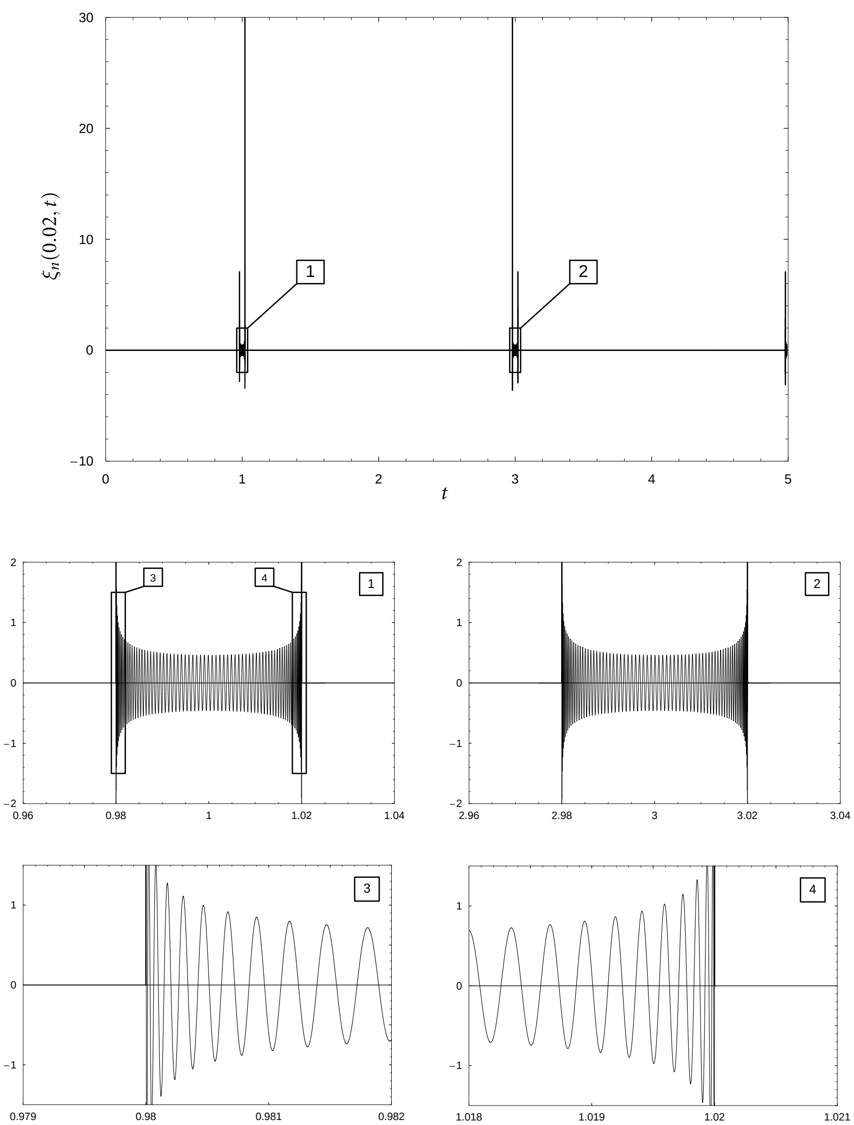

Figure 8: Function $\xi_{150}(0.02, t)$.

https://doi.org/10.4153/CMB-2007-053-1 Published online by Cambridge University Press

ξ_n is the same as that for ψ_n, but all of them have the "mixed" nature with one side limit being finite and the other being infinite. In their intervals of continuity, the functions ξ_n exhibit regular behavior when n is small and r is relatively large. However, as n increases and r decreases, the appearance of ξ_n changes dramatically. Their values become closer and closer to zero in the intervals between any two neighboring points of discontinuity of the same type, and in the intervals formed by the neighboring points of discontinuity of different types, the functions oscillate with frequency that increases significantly as n increases and r decreases, and is much higher in the proximity of the ends of the intervals.

Appendix A $\chi(r, R, \phi)$ on a Circle of a Large Radius

We consider the function

$$\text{(A1)} \qquad \chi(r,R,\phi) = \left\{ \frac{e^{2rR\cos\phi} + e^{-2rR\cos\phi} + 2\sin(2rR\sin\phi)}{e^{2R\cos\phi} + e^{-2R\cos\phi} - 2\sin(2R\sin\phi)} \right\}^{\frac{1}{2}}$$

on the family of circles $R_k e^{i\phi}$ of radius

$$\text{(A2)} \qquad R_k = \pi k, \quad k \gg 1,$$

and we intend to show that χ is uniformly bounded on such a family.

We first consider such values of ϕ that $|\cos\phi| > \delta$, $\delta = \frac{1}{R}$, and assume that $\cos\phi > 0$ (the case of negative $\cos\phi$ can be addressed in a similar manner). Then it is easy to see that

$$e^{2rR\cos\phi} + e^{-2rR\cos\phi} + 2\sin(2rR\sin\phi) < e^{2rR\cos\phi}(1 + e^{-4r} + 2e^{-2r}),$$
$$e^{2R\cos\phi} + e^{-2R\cos\phi} - 2\sin(2R\sin\phi) > e^{2R\cos\phi}(1 - 2e^{-2}).$$

Hence

$$\text{(A3)} \qquad \chi^2 < \frac{(1 + e^{-4r} + 2e^{-2r})}{1 - 2e^{-2}} e^{2(r-1)}.$$

The estimate (A3) allows for analysis of χ as a function of r. For our purposes, however, all we need is to show that χ is bounded on the family (A2). To that end, we can write

$$\text{(A4)} \qquad \chi(r,R,\phi) < \sqrt{2}, \quad \cos\phi > \frac{1}{R}, \quad R \gg 1, \quad r \in [0,1].$$

Note that the estimates (A3) and (A4) are valid for any R, not only for $R = R_k$.

Now we consider the values of ϕ such that $|\cos\phi| \le \delta$, $\delta = \frac{1}{R}$, and assume again that $\cos\phi > 0$. In this case, $\phi = \frac{\pi}{2} - \gamma$, $0 < \gamma \le 2\delta$, and the following asymptotic expressions can be easily obtained,

$$e^{2rR\cos\phi} = e^{2rR\gamma}\left\{1 + O\Big(\frac{1}{R^2}\Big)\right\}, \quad e^{-2rR\cos\phi} = e^{-2rR\gamma}\left\{1 + O\Big(\frac{1}{R^2}\Big)\right\},$$
$$\sin(2rR\sin\phi) = \sin(2rR) + O\Big(\frac{1}{R}\Big).$$

https://doi.org/10.4153/CMB-2007-053-1 Published online by Cambridge University Press

Then the numerator and denominator in (A1) can be estimated as (here we do make use of the fact that $R = R_k = \pi k$)

$$e^{2rR\cos\phi} + e^{-2rR\cos\phi} + 2\sin(2rR\sin\phi) < 3 + e^{4r},$$
$$e^{2R\cos\phi} + e^{-2R\cos\phi} - 2\sin(2R\sin\phi) > \frac{3}{4} + e^{-4},$$

and we have for χ^2,

$$\chi^2 < \frac{4(3 + e^{4r})}{3 + 4\,e^{-4}}. \tag{A5}$$

Again, the right-hand side of (A5) depends on r. We, however, only need to know its maximum value, which occurs when $r = 1$, and the estimate for χ can be written as

$$\chi(r, R, \phi) < 9, \quad 0 < \cos\phi \le \frac{1}{R}, \quad R = R_k = \pi k, \quad k \gg 1.$$

The estimate for negative ϕ can be obtained in a similar manner.

We have therefore demonstrated that $\chi(r, R, \phi)$ is uniformly bounded on any circle of a large enough radius given by (A2).

Appendix B Continuity of I_2

The general term of the series in (9) can be written as

$$\gamma_k = \left\{ \alpha^* + \frac{1}{\sqrt{r}} \cos(\beta_k^n (r-1)) \right\} \left\{ \omega^* + \frac{1}{\pi k} \right\} \{ s^* + \sin(\beta_k^n t) \},$$

where we define α^*, ω^*, and s^* as follows,

$$\alpha^* = \alpha_k^n(r) - \frac{1}{\sqrt{r}} \cos(\beta_k^n (r-1)), \quad \omega^* = \frac{\omega_k^n}{(\omega_k^n)^2 - n^2} - \frac{1}{\pi k},$$
$$s^* = \sin(\omega_k^n t) - \sin(\beta_k^n t).$$

The term γ_k can be expressed as $\gamma_k = \gamma_k^1 + \gamma_k^2$, where

$$\gamma_k^1 = \frac{1}{\sqrt{r}\pi k} \cos(\beta_k^n (r-1)) \sin(\beta_k^n t)$$

is the general term of the series I_1, and

$$\gamma_k^2 = \frac{1}{\sqrt{r}} \cos(\beta_k^n (r-1)) \left\{ \omega^* \sin(\beta_k^n t) + s^* \left\{ \omega^* + \frac{1}{\pi k} \right\} \right\} + \alpha^* \{ s^* + \sin(\beta_k^n t) \} \left\{ \omega^* + \frac{1}{\pi k} \right\}$$

https://doi.org/10.4153/CMB-2007-053-1 Published online by Cambridge University Press

is the general term of I_2. Taking into account the asymptotic expressions (10)–(12), we can easily see that

$$\alpha^* = O\Big(\frac{1}{k}\Big), \quad \omega^* = O\Big(\frac{1}{k^2}\Big), \quad \text{and} \quad s^* = O\Big(\frac{1}{k}\Big),$$

which implies that

$$\gamma_k^2 = O\Big(\frac{1}{k^2}\Big). \tag{B1}$$

Even though we have already known that (B1) was the case, now we have expressed the general term of I_2 in terms of a finite combination of continuous functions. Furthermore, because of the estimate (B1), it is always possible to find large enough N such that I_2 will be uniformly convergent on any finite t-interval (Weierstrass M-test). Then, since γ_k^2 are continuous functions of t, the sum of the uniformly convergent series I_2 is a continuous function as well.

Appendix C Special Case of $r = 0$

The special case of $r = 0$ is quite unique because it corresponds to the zero radial distance in physical applications, and it is quite different from the mathematical point of view as well. For such r,

$$J_n(\omega_k^n r) = \begin{cases} 0 & n \geq 1, \\ 1 & n = 0, \end{cases}$$

for all k, and $\xi_n(0,t) = 0$, $t \geq 0$, for all n except for $n = 0$. If $n = 0$,

$$\xi_0(0,t) = 2t + 2\sum_{k=1}^{\infty} \frac{1}{\omega_k^0 J_0(\omega_k^0)} \sin(\omega_k^0 t). \tag{C1}$$

Since the function (C1) is a limiting case of $\xi_0(r,t)$ when $r \to 0$, the behaviour of $\xi_0(0,t)$ can be assessed based on what we already know about $\xi_0(r,t)$. Specifically, we know that its singularities occur at $t_1^s = 4j - r + 3$ and $t_2^s = 4j + r + 1$, $j = 0, 1, \dots$, and that finite discontinuities occur at $t_1^f = 4j - r + 1$ and $t_2^f = 4j + r + 3$, $j = 0, 1, \dots$. As $r \to 0$, the singularities become closer and closer to the points $4j + 3$ from the left and to the points $4j + 1$ from the right. At the same time, the finite discontinuities are becoming closer and closer to the points $4j + 1$ from the left and the points $4j + 3$ from the right. At $r = 0$, a pair of discontinuities of the two different types merge at each of the points

$$t_m^1 = 4j + 1 \tag{C2}$$

and

$$t_m^2 = 4j + 3, \tag{C3}$$

https://doi.org/10.4153/CMB-2007-053-1 Published online by Cambridge University Press

and the points (C2) and (C3) exhibit a "mixed" nature, *i.e.,* the function $\xi_0(0,t)$ has side limits of different types at those points. Specifically, it has either an infinite left-side limit and a finite right-side one (points t_m^2) or a finite left-side limit and an infinite right-side one (points t_m^1). Figure 9 illustrates these interesting features of $\xi_0(0,t)$.

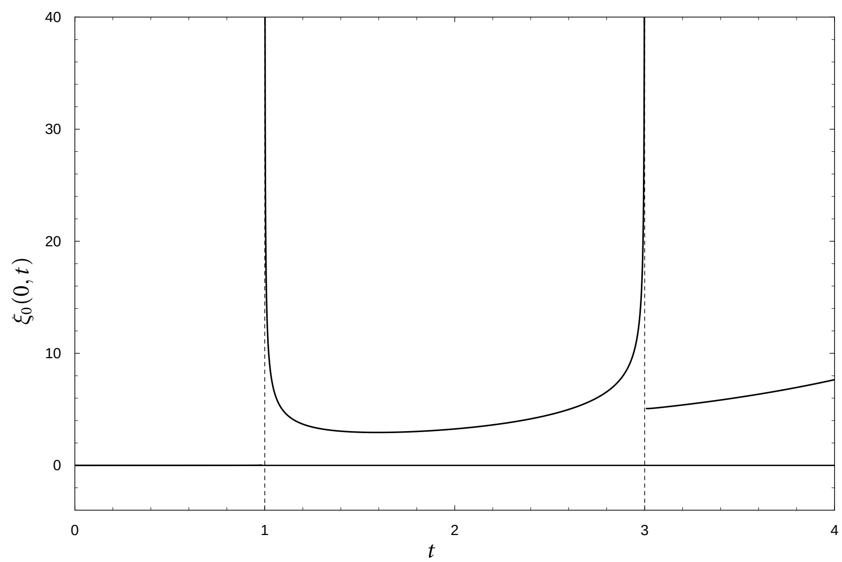

Figure 9: Function $\xi_0(0,t)$.

Acknowledgements The author gratefully acknowledges the financial support of the Natural Sciences and Engineering Research Council (NSERC) of Canada (Discovery Grant 261949), the Killam Trusts, and the Faculty of Engineering, Dalhousie University.

References

[1] M. Abramowitz and I. A. Stegun, *Handbook of Mathematical Functions: with Formulas, Graphs and Mathematical Tables.* Dover, New York, 1965.

[2] A. Erdelyi, W. Magnus, F. Oberhettinger, and F. G. Tricomi, *Higher Transcendental Functions.* Vol. 1, McGraw-Hill, New York, 1953.

[3] ———, *Higher Transcendental Functions.* Vol. 2, McGraw-Hill, New York, 1953.

[4] T. L. Geers, *Excitation of an elastic cylindrical shell by a transient acoustic wave.* J. Appl. Mech. **36**(1969), 459–469.

[5] ———, *Scattering of a transient acoustic wave by an elastic cylindrical shell.* J. Acoustical Soc. Amer. **51**(1972), 1640–1651.

[6] S. Iakovlev, *Interaction of a spherical shock wave and a submerged fluid-filled circular cylindrical shell.* J. Sound Vibration **225**(2002), 615–633.

[7] ———, *On the singular behavior of the inverse Laplace transforms of the functions $I_n(s)/(sI_n'(s))$.* Canad. Math. Bull. **45**(2002), no. 3, 399–416.
[8] ———, *Influence of a rigid co-axial core on the stress-strain state of a submerged fluid-filled circular cylindrical shell subjected to a shock wave.* J. Fluids Structures **19**(2004), no. 7, 957–984.
[9] ———, *Hydrodynamic shock loading on a submerged fluid-filled cylindrical shell.* J. Fluids Struct. **22**(2006), no. 8, 997–1028.
[10] H. U. Mair, *Benchmarks for submerged structure response to underwater explosion.* Shock and Vibration **6**(1999), 169–181.

Department of Engineering Mathematics and Internetworking
Dalhousie University
Halifax, NS
B3J 2X4
e-mail: serguei.iakovlev@dal.ca